

LETTERS

Controlled Size, Nanometer-Scale, Reaction Vessels in Two Dimensions

Kourosh Nafisi, Jeffrey Samu, and John C. Hemminger*

Department of Chemistry and Institute for Surface and Interface Science, University of California, Irvine, California 92697-2025

Received: July 20, 2000; In Final Form: September 22, 2000

Islands of monolayer vacancies can be generated on transition metal surfaces by ion bombardment of samples held at elevated temperature. Our experiments show that the average size of the monolayer vacancy islands can be varied in a controlled manner from 3 to 30 nm by adjusting the sample temperature. We also demonstrate that monolayer vacancy islands can be used as two-dimensional nanometer-scale catalytic "reaction vessels." The reactants are confined to the reaction vessels by energetic barriers to adsorbate diffusion across the atomic steps that form the walls of the vessels. Reaction vessels with diameters of ~ 3 nm can accommodate only a small number of reactant molecules (e.g., a maximum of 28 ethylene molecules can be adsorbed in an area with a diameter of 3.3 nm on a Pt(111) surface). Reactions whose products or rates depend on the number of reactant molecules that are available can be controlled using these reaction vessels. This is demonstrated for the particular example of carbon particles that are formed from the dehydrogenation of mono-olefins on Pt.

Introduction

The development of experimental methods to carry out chemical reactions on the nanometer scale has become of tremendous interest in recent years. In this paper, we describe experiments which show that we can combine two phenomena to confine molecules within the nanometer scale, catalytically active reaction vessels, and observe subsequent reactions. The two phenomena that underlie our experiments are:

- (1) Molecular adsorbates on transition metal surfaces exhibit energetic barriers to diffusion across monatomic steps.
- (2) Controlled ion sputtering of a surface can be used to decorate a metal surface with monolayer vacancy islands (single atomic layer deep holes) of controllable size that can be used as "reaction vessels".

We also show that on the nanometer scale, the outcome of reactions depends on the size of the reaction vessel.

The confinement of molecular adsorbates to nanometer-scale regions on surfaces has been accomplished in the past by constructing "molecule corrals". In those nonreactive experiments, confinement regions have been generated atom by atom at low temperature (4 K) using a scanning tunneling microscope (STM) or by generating pits on graphite surfaces using oxidation methods.¹⁻³ In addition, Hooks et al., have demonstrated nanoconfined electrochemical nucleation in pits on graphite surfaces.⁴ Our experiments show that nanometer-scale reaction vessels can be constructed with size control on catalytically active transition metal surfaces.

Bombardment of transition metal surfaces with rare gas ions, often referred to as sputtering, is well known to remove atoms from the metal surface. Comsa and co-workers⁵ have shown that the sputtering of a Pt(111) surface with the surface held at elevated temperature results in the decoration of the surface with islands of monolayer vacancies. They have also discussed the mechanism of monolayer vacancy island formation in detail.^{5b-e} We show here that careful control of the sample temperature

* Corresponding author. E-mail: jchemmin@uci.edu.

can result in relatively narrow size distributions of the resulting monolayer vacancy islands. By observing the carbon particles that are produced by the dehydrogenation of mono-olefins on Pt surfaces with reaction vessels of various sizes, we further demonstrate that the size of the vacancy island reaction vessels can impact the outcome of surface reactions.

Experimental Section

The experiments described here were carried out in an ultrahigh vacuum chamber equipped with an Auger electron spectrometer (Physical Electronics single-pass cylindrical mirror analyzer), low-energy electron diffraction optics (Physical Electronics LEED optics), mass spectrometry capabilities (UTI 100C), and a variable temperature “beetle”-style scanning tunneling microscope.⁶ The ion bombardment was carried out utilizing a differentially pumped rare-gas ion gun (Physical Electronics Model 04303A). Details of the instrument, including the variable-temperature STM, have been published previously.^{7a,b} All images shown here were obtained with the typical tunneling conditions of 1 namp tunneling current and 0.50 V bias. Adsorbate gases were introduced to the chamber via sapphire-sealed leak valves. One of the leak valves was equipped with a tube-type doser that allowed gas exposure to the sample while limiting the background pressure increase.

Results and Discussion

Generation of Nanometer-Scale 2-D Reaction Vessels.

Figure 1 shows an STM image of a Pt(111) surface immediately after the sample was sputtered with Ar⁺ ions of 600 eV, with the sample held at 775 K during the ion bombardment. Figure 1 shows that this sample preparation generates a surface which has been decorated with relatively large monolayer vacancy islands (mean diameter, $\sim 32 \pm 14$ nm) with a fairly broad size distribution (shown in Figure 1b). The monolayer vacancy islands generated in this manner are stable over long periods of time as long as the sample temperature is kept below ~ 600 K, and they are even stable for short periods at temperatures as high as 800 K. The monolayer vacancy islands can be removed by annealing at temperatures in excess of 800 K for extended periods. Figures 2–4 show how the sizes of the monolayer vacancy islands change as a function of the temperature of the sample during ion bombardment. Bombardment of the sample at 725 (Figure 2), 675 (Figure 3), and 625 K (Figure 4) generate monolayer vacancy islands with mean diameters of 12.8 ± 5 , 7.2 ± 2 , and 3.3 ± 1 nm, respectively. If the sample is held at temperatures significantly below 625 K during ion bombardment under otherwise identical sputtering conditions, the resulting sample morphology will be quite different. Under such conditions, multilayer-deep vacancy islands are generated. Multilayer vacancy islands may be useful for the confinement of chemistry in special cases but will not be considered further here.

Monolayer vacancy islands have been generated on a variety of transition metal surfaces.^{5,8–11} The appropriate temperatures for preparing different sizes of vacancy islands will scale with the substrate melting temperature since the preparation process involves a tradeoff between the efficiency of atom removal by sputtering and the rate of substrate atom diffusion on the surface. As described in detail by Michely et al.,⁵ the 3-fold symmetrical shape of the vacancy islands (e.g., Figure 1) is the result of 3-fold symmetry of the Pt(111) substrate. Other symmetry surfaces can be used to generate alternate shapes (e.g., fcc(100) surfaces to generate square shapes and fcc(110) surfaces to generate rectangular shapes).

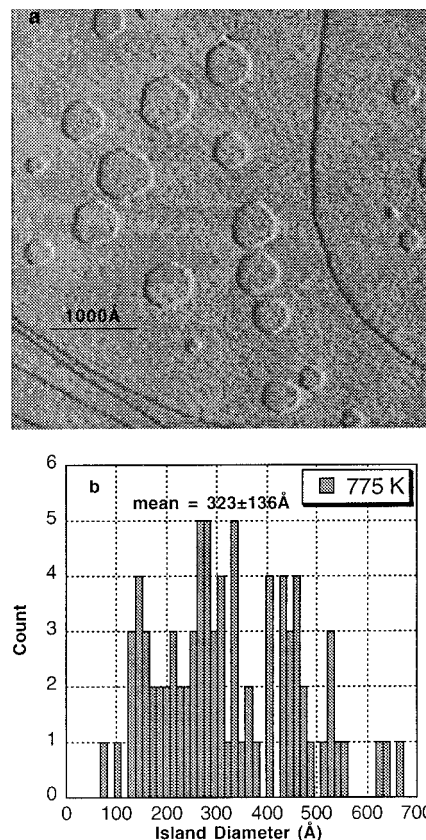


Figure 1. Monolayer vacancy islands generated on a Pt(111) surface by ion bombardment of the sample with 600 eV Ar⁺ ions while the sample was held at 775 K. (a) A $4860 \text{ Å} \times 4860 \text{ Å}$ “differentiated” STM image of the surface after ion bombardment. (b) A plot of the distribution of diameters of monolayer vacancy islands resulting from ion bombardment at 775 K. The mean diameter of the monolayer vacancy islands produced under these conditions is $320 \pm 136 \text{ Å}$. The data for this plot were obtained by analyzing STM images, such as that shown in (a), from different areas of the sample surface.

Reactions in Nanometer-Scale 2-D Reaction Vessels. As we point out in the Introduction, the ability to generate nanometer-scale vacancy islands allows us to modify chemical reactions by confining the reactants to catalytic reaction vessels of varying size. Surface diffusion in and out of the vessel will be limited due to the enhanced energetic barriers for diffusion across the steps that make up the edges of the vessels. Enhanced energetic barriers to the self-diffusion of adsorbate atoms across steps (so-called Ehrlich-Schwoebel barrier) have been demonstrated both experimentally and theoretically for a number of atomic adsorbate systems.^{12–17} While less quantitative data is available for the diffusion of molecular adsorbates on surfaces, ample evidence suggests that similar enhanced energetic barriers to diffusion across steps exist for molecular adsorbates.¹⁸

The impact of this confinement phenomenon can be understood by considering how many molecules will actually fit in a nanometer-scale monolayer vacancy island. The adsorption of a relatively small molecular adsorbate, ethylene, on Pt(111) has been studied in great detail.¹⁹ It is known that on Pt(111), one ethylene molecule can adsorb for every four surface Pt atoms.²⁰ Thus, a surface reaction vessel of 32 nm diameter may contain as many as 2600 ethylene molecules—quite a large number on the scale of a chemical reaction. However, a 3.3 nm diameter reaction vessel (such as those shown in Figure 4) can contain at most 28 ethylene molecules. Thus, if the products or the rate of a reaction depends critically on the number of reactant molecules available in the reaction vessel, the predicted outcome

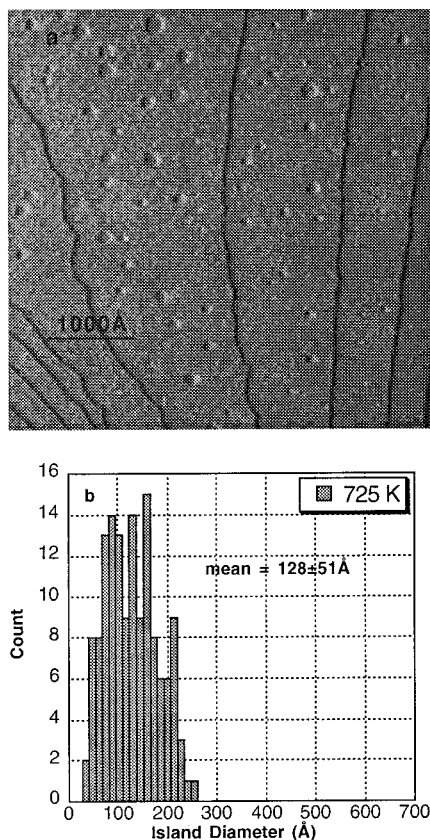


Figure 2. Monolayer vacancy islands generated on a Pt(111) surface by ion bombardment of the sample with 600 eV Ar^+ ions while the sample was held at 725 K. (a) A $4860 \text{ Å} \times 4860 \text{ Å}$ “differentiated” STM image of the surface after ion bombardment. (b) A plot of the distribution of diameters of monolayer vacancy islands resulting from ion bombardment at 725 K. The mean diameter of the monolayer vacancy islands produced under these conditions is $128 \pm 51 \text{ Å}$. The data for this plot were obtained by analyzing STM images, such as that shown in (a), from different areas of the sample surface.

can vary tremendously over the range of nanometer-scale reaction vessels that we can produce.

An obvious class of reactions to consider would be polymerization reactions. A simple example that we show here involves the catalytic dehydrogenation of ethylene on Pt. The initial step in the catalytic dehydrogenation of ethylene on Pt(111) results in the formation of ethylidyne ($\text{C}=\text{CH}_3$).¹⁹ In previous studies, we have shown that further catalytic dehydrogenation of ethylidyne results in the aggregation of partially dehydrogenated carbonaceous fragments to form particles.²¹ We have shown that other mono-olefins also produce particles in the same manner upon catalytic dehydrogenation on Pt(111).^{7a} Heating the sample to temperatures of $\sim 700 \text{ K}$ results in complete hydrogen removal, producing carbon particles. The carbon particles have a quite narrow size distribution and are approximately 1 nm in diameter, with ~ 35 carbon atoms per particle.²¹ For ~ 35 carbon atoms to be provided in a single particle, dehydrogenation and aggregation of ~ 18 ethylene molecules is required. One complication presented by the very small reaction vessels is that the mobile carbonaceous fragments which aggregate to form carbon particles would also be expected to bond to the walls of the reaction vessel. That is, the fragments will bind more strongly to the coordinatively unsaturated Pt atoms at the steps that form the walls of the reaction vessels. For large reaction vessels, this is a negligible effect; however, for smaller reaction vessels, this depletes the reactant significantly and must be taken into account when considering the

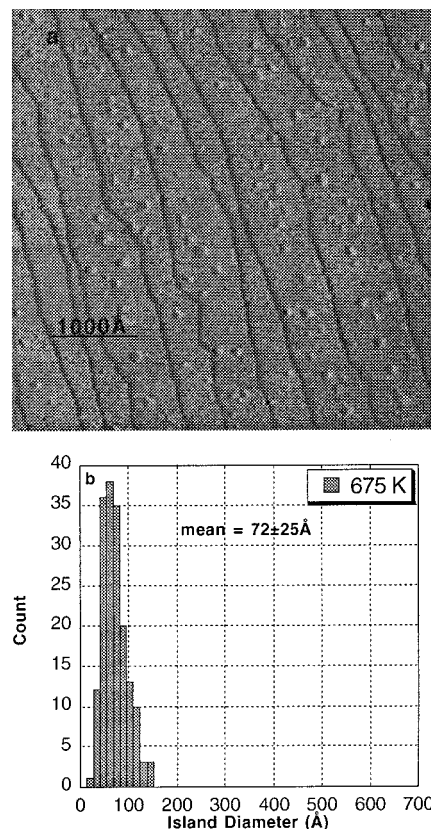


Figure 3. Monolayer vacancy islands generated on a Pt(111) surface by ion bombardment of the sample with 600 eV Ar^+ ions while the sample was held at 675 K. (a) A $4860 \text{ Å} \times 4860 \text{ Å}$ “differentiated” STM image of the surface after ion bombardment. (b) A plot of the distribution of diameters of monolayer vacancy islands resulting from ion bombardment at 675 K. The mean diameter of the monolayer vacancy islands produced under these conditions is $72 \pm 25 \text{ Å}$. The data for this plot were obtained by analyzing STM images, such as that shown in (a), from different areas of the sample surface.

outcome of the reaction. If the density of fragments required to passivate the walls of the reaction vessels is assumed to be the same as the adsorption density of ethylene on Pt(111) (a linear density of 1 ethylene for every 2 Pt atoms), the number of fragments required to passivate the walls of a reaction vessel will be $\pi d / (0.277 \cdot 2)$, where 0.277 nm is the Pt–Pt spacing. For a 3.3 nm diameter reaction vessel, ~ 19 ethylene molecules would be required to passivate the walls of the vessel in competition with the formation of carbon particles. This would leave only 9 ethylene molecules in the reaction vessel—a factor of 2 less than required to form the carbon particles we have observed in previous experiments. This calculation can easily be inverted to predict that particles would not be formed in reaction vessels with diameters less than approximately 4 nm and would be formed in larger reaction vessels.

To test this concept, we generated a Pt(111) surface that was decorated with reaction vessels having a mean diameter of approximately 7 nm (i.e., ion bombardment at $\sim 675 \text{ K}$). The distribution we obtain (see Figure 3) would then contain many reaction vessels that are larger than the expected critical size of $d = 4 \text{ nm}$ but also some smaller reaction vessels with diameters less than the critical value. We then adsorbed 1-butene at saturation coverage and heated the sample to $\sim 700 \text{ K}$ to completely dehydrogenate the butene and form carbon particles. The STM image in Figure 5 shows that particles are observed on the Pt(111) terraces and in the larger of the monolayer vacancy islands. The particle density and size are consistent with the amount of carbon in the molecular monolayer, as we

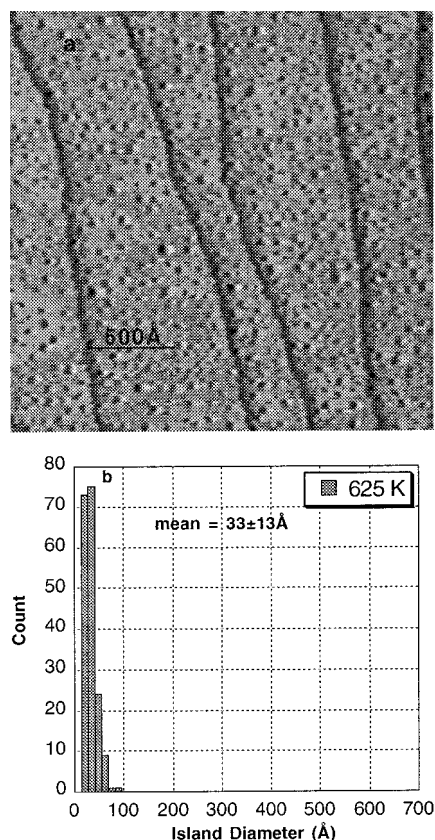


Figure 4. Monolayer vacancy islands generated on a Pt(111) surface by ion bombardment of the sample with 600 eV Ar^+ ions while the sample was held at 625 K. (a) A $2430 \text{ Å} \times 2430 \text{ Å}$ “differentiated” STM image of the surface after ion bombardment. (b) A plot of the distribution of diameters of monolayer vacancy islands resulting from ion bombardment at 625 K. The mean diameter of the monolayer vacancy islands produced under these conditions is $33 \pm 13 \text{ Å}$. The data for this plot was obtained by analyzing many STM images such as the one shown in (a), from different areas of the sample surface.

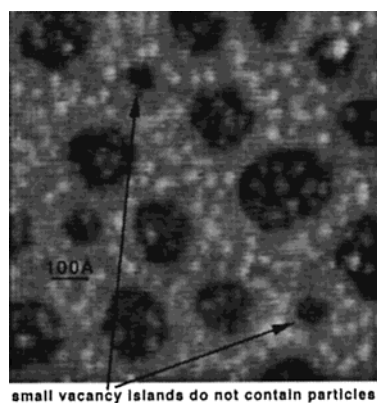


Figure 5. A $608 \text{ Å} \times 608 \text{ Å}$ raw data STM image of the Pt(111) surface after decoration with monolayer vacancy islands by bombardment at 675 K followed by the dehydrogenation of 1-butene to form carbon particles. The carbon particles are presented as the small white dots in the figure on the extended terraces and inside the larger monolayer vacancy islands but not inside the smaller monolayer vacancy islands. Analyzing many images of this kind leads to a critical diameter of 5 nm. Vacancy islands larger than this critical value contain carbon particles, whereas smaller vacancy islands do not.

have described in detail previously.²¹ However, the smaller-monolayer vacancy islands never show carbon particles. The critical size that we observed in this experiment is 5.0 nm. That is, monolayer vacancy islands with diameters greater than 5.0 nm are always observed to contain carbon particles, whereas

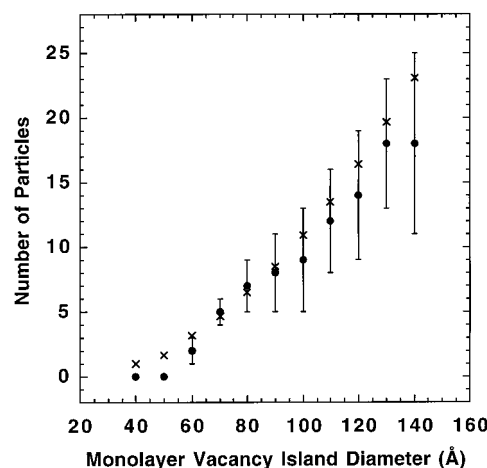


Figure 6. Plot of the number of carbon particles found within monolayer vacancy islands as a function of the diameter of the island. The solid points are averages of the number of carbon particles observed in islands within $\pm 5 \text{ Å}$ of the plotted diameter. The error bars represent the standard deviations in the plotted averages. The \times 's indicate the value expected on the basis of the model present in the text.

those with diameters less than 5.0 nm never contain carbon particles. This is in quite good agreement with the simple model, which predicts a critical diameter of $\sim 4 \text{ nm}$. Figure 6 shows a plot of the number of particles found in a given size vacancy island as a function of island size. Since, in this experiment, we utilized a vacancy island size distribution similar to that shown in Figure 3; the statistics (indicated by the error bars in the plot) are best for islands with a diameter of $\sim 70 \text{ Å}$ at the peak of the distribution. The number of particles expected on the basis of the simple model is also shown in the plot of Figure 6. The results from the experiments are in quite good agreement with the simple model. Thus, the monolayer vacancy islands are indeed acting as nanometer-scale catalytic reaction vessels in two dimensions.

Conclusions

Our experiments demonstrate that Pt surfaces can be decorated with nanometer-scale monolayer-deep vacancy islands and that these vacancy islands can act as two-dimensional reaction vessels that confine reactants and products during a thermally activated catalytic reaction. Moreover, we have demonstrated the ability to generate such reaction vessels while controlling the diameters in the range from ~ 3 to $\sim 30 \text{ nm}$ with narrow size distributions for the smaller reaction vessels ($d \leq 10 \text{ nm}$). This level of control opens the possibility of controlling the course of a wide range of reactions on catalytically active metal surfaces. It is likely that we will be able to modify other classes of chemical reactions by confining the reactants and products in nanometer-scale reaction vessels such as those described here. We have, for example shown, that the kinetics of surface reactions can depend on the spatial arrangement of reactants and products²² especially in systems that exhibit adsorbate island formation. Such reaction systems could be substantially modified by the confinement effects we demonstrate here. It is also likely that reaction vessels of different shape (e.g., square or rectangular) will have significant effects on the outcome of the reaction.

Acknowledgment. This work was supported in part by the Department of Energy under Grant DE-FG03-96ER45576. J.C.H. thanks the Alexander von Humboldt Foundation and the Fritz-Haber Institute der Max-Planck-Gesellschaft for financial

support, as well as scientific discussions and hospitality during the preparation of this manuscript.

Note Added after ASAP Posting

This article was posted ASAP with an error in the title on 10/14/2000. The corrected version was posted on 12/8/2000.

References and Notes

- (1) Crommie, M. F.; Lutz, C. P.; Eigler, D. M. *Science* **1993**, 262, 218.
- (2) Chang, H.; Bard, A. J. *J. Am. Chem. Soc.* **1991**, 113, 5588.
- (3) Patrick, D. L.; Cee, V. J.; Beebe, T. P., Jr. *Science* **1994**, 265, 231.
- (4) Hooks, D. E.; Yip, C. M.; Ward, M. D. *J. Phys. Chem. B* **1998**, 102, 9958.
- (5) (a) Michely, T.; Comsa, G. *Nucl. Instrum. Methods Phys. Res., Sect. B* **1993**, 82, 207. (b) Michely, T.; Land, T.; Comsa, G. *Phys. Rev. Lett.* **1992**, 272, 204. (c) Poelsema, B.; Verheji, L. K.; Comsa, G. *Phys. Rev. Lett.* **1984**, 53, 2500. (d) Poelsema, B.; Kunkel, R.; Verheji, L. K.; Comsa, G. *Phys. Rev., B* **1990**, 41, 11609. (e) Michely, T.; Comsa, G. *Surf. Sci.* **1991**, 256, 217. (f) Bott, M.; Michely, T.; Comsa, G. *Surf. Sci.* **1992**, 272, 161.
- (6) Frohn, J.; Wolf, J. F.; Besocke, K.; Teske, M. *Rev. Sci. Instrum.* **1989**, 60, 1200.
- (7) (a) Nafisi, K., Ph.D. Dissertation, University of California, Irvine, CA, 2000. (b) Nafisi, K.; Raunau, W.; Hemminger, J. C. *Rev. Sci. Instrum.*, in press.
- (8) Rusponi, S.; Borango, C.; Ferrando, R.; Hontinfinde, F.; Valbusa, U. *Surf. Sci.* **1999**, 440, 451.
- (9) Rosenfeld, G.; Morgenstern, K.; Esser, M.; Comsa, G. *Appl. Phys. A* **1999**, 69, 489.
- (10) Malafsky, G. P. *Surf. Sci.* **1994**, 306, L539.
- (11) Morgenstern, K.; Rosenfeld, G.; Poelsema, B.; Comsa, G. *Phys. Rev. Lett.* **1995**, 74, 2058.
- (12) Schwoebel, R. L.; Shipsey, E. J. *J. Appl. Phys.* **1966**, 37, 3682.
- (13) Ehrlich, G.; Hudda, F. G. *J. Chem. Phys.* **1966**, 44, 1039.
- (14) Giesen, M.; Ibach, H. *Surf. Sci.* **1999**, 431, 109.
- (15) Feibelman, P. J. *Phys. Rev. Lett.* **1998**, 81 (1), 168.
- (16) Feibelman, P. J. *Phys. Rev. B* **1999**, 60 (7), 4972.
- (17) Sneh, O.; George, S. M. *J. Chem. Phys.* **1994**, 101 (4), 3287.
- (18) Avena, M. V.; Westre, E. D.; George, S. M. *J. Chem. Phys.* **1992**, 96 (1), 808.
- (19) Carter, E. A.; Koel, B. E. *Surf. Sci.* **1990**, 226, 339.
- (20) Land, T. A.; Michely, T.; Behm, R. J.; Hemminger, J. C.; Comsa, G. *Appl. Phys. A* **1991**, 53, 414.
- (21) Land, T. A.; Michely, T.; Behm, R. J.; Hemminger, J. C.; Comsa, G. *J. Chem. Phys.* **1992**, 97, 6774.
- (22) Erley, W.; Li, Y.; Land, D. P.; Hemminger, J. C. *Surf. Sci.* **1994**, 301, 177.